EXPERIMENTAL INVESTIGATION AND MODELING OF THE BEHAVIOR OF COMMINGLED YARNS

J.E Rocher[a*], S. Allaoui[a], G. Hivet[a], E. Blond[a]

[a]*Laboratoire PRISME/MMH, Université d'Orléans, 8 rue Léonard de Vinci, 45072 Orléans Cedex 2, France.*
** jean-emile.rocher@univ-orleans.fr*

Keywords: experimental testing, tensile behavior, commingled yarns, modeling.

Stress-strain tensile behavior of commingled glass-fiber/polypropylene yarns is experimentally investigated. Values of Young modulus, breaking stress and breaking strain of yarns and their dependence to strain rate and gauge length are evaluated. A comparison of tensile behavior of yarns before and after weaving of a 3D-fabric is performed in order to estimate the influence of weaving damage. Taking into account the particular commingled yarn structure, a model is proposed to describe accurately their full stress-strain tensile behavior. Parameters of the model are identified in the light of experimental results.

1. Introduction

Several textile-reinforced composite parts manufacturing processes requires the forming of reinforcements into the desired shape. Apparition of defects on the reinforcement during this process can significantly decrease mechanical properties of the final composite part [1-3]. Experimental characterization tests have been developed in order to investigate deformability of dry fabrics but they are costly and difficult to perform. Meso-scale simulations can be used to investigate deformability of fabrics by performing finite element analyses on CAD models of the fabric unit cell. To perform realistic meso-scale simulations on commingled yarns made fabrics, it is important to investigate and model accurately these yarns mechanical behavior. In particular, their specific tensile behavior must be considered. To do so, it is necessary to perform tensile tests and to build a model describing the stress-strain tensile behavior of these yarns.

In this study, the tensile behavior of commingled polypropylene/glass yarns is investigated; influence of gauge length and strain rate are evaluated. A comparison of tensile behavior of yarns before and after weaving of a 3D-fabric is performed in order to estimate the influence of weaving damage. Taking into account the particular structure of commingled yarns, a model describing their stress-strain behavior is proposed. Parameters of this model are identified, paving the way to meso-scale simulations on commingled yarns made fabrics.

2. Materials and methods

2.1. Materials

Commingled yarns used in this study were obtained by an air-jet texturing technique: reinforcement and matrix input yarns filaments are mixed together using an air-nozzle. Use of over-delivery is necessary to perform the commingling but must be as low as possible especially for reinforcement fibers to avoid important loss of orientation [4]. Structure of commingled yarns is highly influenced by the air jet texturizing process that leads to the apparition of opened areas and nips along the yarn length (see Figure 1). Previous studies [5-7] have shown that the number, type, repartition and stability of nips and therefore the commingled yarn tensile behavior itself are highly influenced by the chosen commingling parameters such as commingling speed, pressure, delivery values. Commingled yarns studied here (that will be referred as GFPP yarns in the following) were obtained using as input a 300 tex E-glass fiber (GF) yarn and 3*32 tex polypropylene (PP) yarns with an overdelivery (OD) of 2 % for GF and 5% for PP. More details concerning the commingling process can be found in [8]. Final yarn count is approximately 410 tex for a glass fiber volume fraction $V_{GF} = 52\%$.

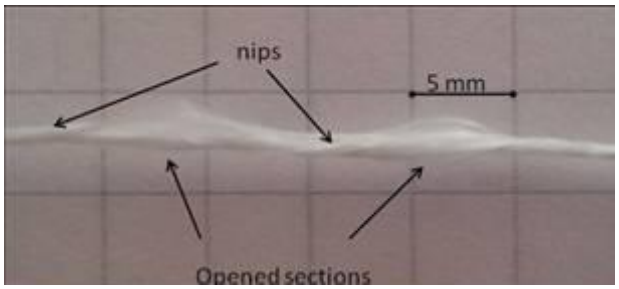

Figure 1. Global structure of a commingled yarn

Within European project 3D Light-trans, commingled yarns have been used to produce 3D fabrics. Weaving configuration of one of these fabrics is shown Figure 2. It is composed of five layers of yarns in the weft direction (grey) and four in the warp direction (red). Binding yarns are vertically oriented and interlock 3 layers of weft yarns. The weaving density of fabric is 240 yarns/10cm for weft yarns and 200 yarns/10cm for both warp yarns and binding yarns. All yarns used in the fabric are the previously described GFPP yarns.

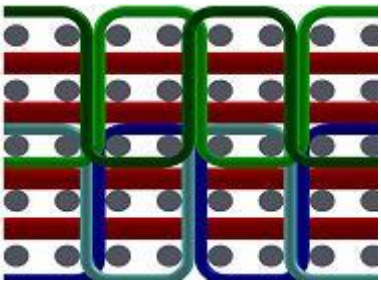

Figure 2. Weaving configuration of the 3D fabric

2.2. Methods

Yarn tensile tests were performed with 2 gauge length of 200 and 500 mm and at three strain rates of $1.67*10^{-4}$ s^{-1} (quasi static loading), $1.67*10^{-3}$ s^{-1} and $1.67*10^{-2}$ s^{-1}. Tests were performed using a universal testing machine (INSTRON 4507). Samples were prepared by fixing yarns between thin aluminum plates with glue. At least 10 tests were performed in each

testing configuration, more when an important scattering of tensile behavior between samples was highlighted. A 5mN/tex preload was used.

3. Experimental results

The typical quasi-static ($1.67*10^{-4}$ s^{-1} strain rate) stress-strain tensile behavior of a GFPP yarn is shown Figure 3. An initial non linear behavior with a gradual increase of yarn stiffness is observed (up to ε_{NL}). Yarn behavior then becomes linear, still, little drops of force corresponding to the opening of unstable nips can be observed. Behavior remains almost linear up to the brutal break of GF, and then the load is taken up by PP [7].

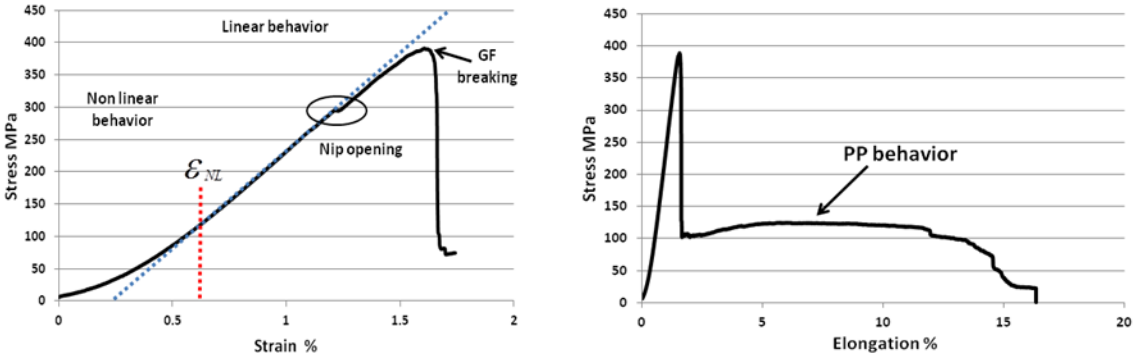

Figure 3. Left: first part of GFPP yarn tensile behavior. Right: Global GFPP tensile behavior

An important scattering of tensile properties from one sample to the other is observed: coefficient of variation of measured breaking stress, breaking strain and Young modulus is more than 10%. In quasi-static loading conditions, for the 200 mm gauge length, average breaking stress is of 340 MPa corresponding to a breaking strength of 80 N. Breaking strain is approximately 1.5 %. Average Young's modulus (measured in the linear part of the stress-strain curve) is close to 30 GPa.

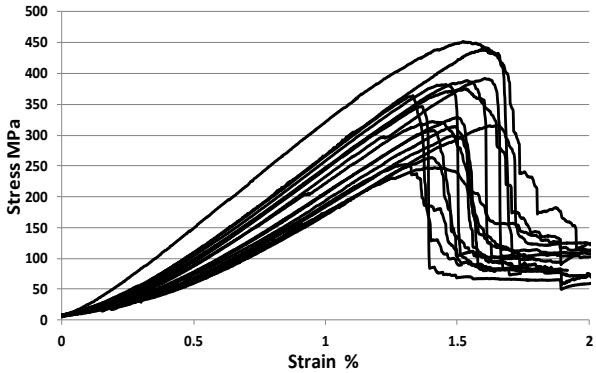

Figure 4. Scattering of GFPP yarns tensile behavior (200mm gauge length, $1.67*10^{-4}$ s^{-1} strain rate)

Average GFPP stress-strain curves for the 200mm gauge length at the 3 strain rates are shown on Figure 5. First parts of the stress-strain curves are almost superposed for the 3 strain rate. For the two gauge lengths, the average breaking strength at $1.67*10^{-2}$ s^{-1} strain rate is 60% higher than the one measured at $1.67*10^{-4}$ s^{-1}. For the $1.67*10^{-4}$ s^{-1} strain rate, average

breaking strength is approximately 6% higher with the 200mm gauge length than with the 500 mm gauge length. This difference seems to increase slightly with strain rate (13% difference at $1.67*10^{-2}$ s^{-1} strain rate). Young's modulus seems to increase slightly with strain rate and to decrease slightly with gauge length.

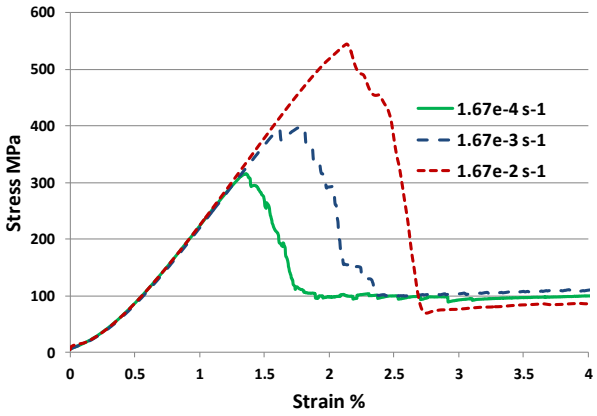

Figure 5. Average stress-strain tensile behavior of GFPP yarns for the 3 strain rates (200 mm gauge length)

Studies [14] have shown that during the weaving process, yarn can be importantly damaged. In order to quantify the damage on the commingled yarns during the 3D-fabric weaving, weft, warp and binding yarns were extracted from the fabric and tested (with gauge length 200mm and strain rate $1.67*10^{-4}$ s^{-1}).

Measured breaking stress, breaking strain and modulus obtained for the 3 groups of yarns extracted are shown Table1. Difference between these values and the one obtained with yarns before the weaving process are reported in parenthesis. A decrease of breaking strength is observed for all the yarns extracted from the fabric. Modulus of warp direction yarns (warp and binding yarns) is not decreased. Weft yarns are the most damaged, with a decrease of 28 % of breaking stress and also a reduction of modulus (-17%). A very important scattering of measured breaking stress and modulus is observed for weft yarns. Observations show that on some samples fibers have been broken by the weaving process, explaining the decreased breaking stress and modulus.

	Breaking strain [%]	Breaking stress [MPa]	Modulus [GPa]
Binding yarns	$1.24^{\pm 0.15}$ (-16 %)	$290^{\pm 38}$ (-15 %)	$29.4^{\pm 2.7}$ (+ 1 %)
Warp yarns	$1.21^{\pm 0.13}$ (-17 %)	$266^{\pm 35}$ (-22 %)	$28.2^{\pm 2.0}$ (- 3 %)
Weft yarns	$1.31^{\pm 0.15}$ (-11 %)	$244^{\pm 90}$ (-28 %)	$24.2^{\pm 8.3}$ (- 17 %)

Table 1. Mechanical parameters of yarns extracted from 3D fabric and comparison with values obtained with yarns before the weaving process in parenthesis.

4. Modeling

The purpose of this part is to model the stress-strain tensile behavior of commingled yarns. First goal is to explain the initial non linear behavior. Main contribution to the tensile behavior of commingled yarns during the initial stage (Figure 3. Left) can be attributed to

glass fibers, their modulus being much higher than PP fibers modulus. As seen Figure 1, due to the commingling process, waviness of fibers can be observed in the commingled yarn structure. During loading, it can be supposed that fibers will progressively align along the yarn direction. Of course this reorganization mechanism will be strongly linked to the intermingling of fibers in nips. In [13] a model taking into account slack of fibers in the case of rovings has been proposed and validated. The slack of filament i being noted θ_i , when a roving of length L is submitted to a displacement u the deformation of fiber i can be written [13]:

$$\varepsilon_i = \frac{e-\theta_i}{1+\theta_i} \tag{1}$$

with $e = u/L$ the yarn deformation. Assuming a linear-elastic, brittle response of fibers of modulus E and a large number of fibers in the roving, the stress-strain behavior can be expressed by:

$$\sigma_\theta(e) = E\int_\theta \frac{e-\theta}{1+\theta} dG_\theta(\theta) \tag{2}$$

With $G_\theta(\theta)$ the cumulative density of delayed activation that can be extracted from experimental results by constructing the normalized derivative of the stress-strain curve.

It is interesting to see if this model can be used to describe the initial non linear behavior of commingled yarns since their particular structure leading to the waviness of filaments can be supposed to act as a slack of fibers. Modulus of the GFPP yarns is referred as E_{GFPP} , model to estimate its value can be found in [4]. Using piecewise linear functions, the shape of the normalized derivative of the stress-strain curve is fitted to obtain an estimation of $G_\theta(\theta)$. Stress-strain tensile behavior is deduced using Equation 2 and shows a very good agreement with experimental results.

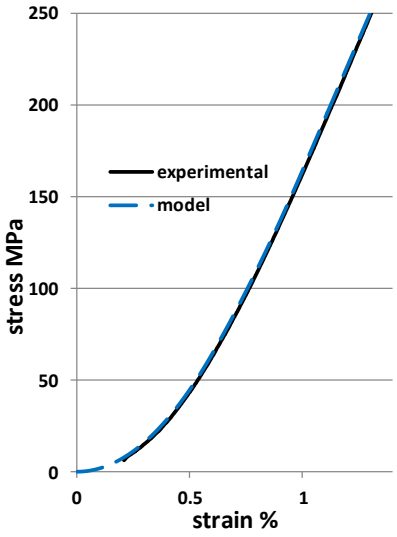

Figure 6. Initial non linear behavior: model/ experimental results comparison

For yarns before the weaving process, experimental results show that the initial non linear behavior is not influenced by strain rate (see Figure 5) and gauge length. Parameters identified can be used to describe the tensile behavior up to linear behavior phase just taking into account the slight variations of E_{GFPP} value with strain rate and gauge length. For yarns extracted from the fabric (whose behavior corresponds to the real yarn behavior that must be considered in simulations), experimental results show that the initial non linear behavior is only slightly influenced by the weaving process, it is therefore just necessary to take into account the decreased E_{GFPP} value for weft yarns.

Weibull models have been widely used [10-12] and are well adapted to describe roving tensile behavior. They are based on the assumptions that the fiber behavior is brittle linear-elastic and that failure probability of single fibers under tension follows a Weibull distribution. For a roving of length L, the stress-strain curve is given by Equation 3.

$$\sigma(e) = Ee \times \exp^{-L\left(\frac{e}{e_0}\right)^m} \tag{3}$$

With e_0 and m parameters identified to fit with experimental data. Same kind of model can be used to describe the average GFPP tensile behavior. The full stress-strain behavior can be modeled by:

$$\sigma(e) = \sigma_\theta(e) \times \exp^{-L\left(\frac{e}{e_0}\right)^m} + \sigma_{PP}\left(1 - \exp^{-L\left(\frac{e}{e_0}\right)^m}\right) \tag{4}$$

$\sigma_\theta(e)$ is the previously identified model describing the stress-strain curve up to linear behavior. Second part of the equation describes the fact that load is taken up by PP fibers when a GFPP yarn breaks. e_0 and m are here linked to the scattering of tensile properties of GFPP yarns. Parameters values $\sigma_{PP} = 100\ MPa$ $e_0 = 0.0164$ and $m = 17$ have been identified on results obtained for yarns before the weaving process in testing configuration (200mm gauge length-1.67*10^{-4} s^{-1} strain rate). An accurate description of the full average stress-strain behavior is obtained as seen Figure 7.

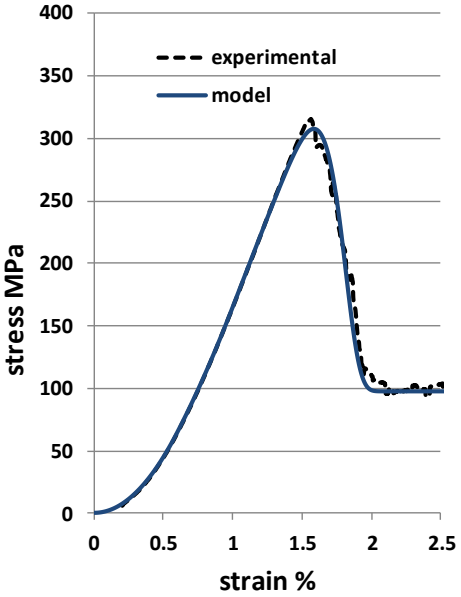

Figure 7. Average tensile behavior: model/ experimental result comparison

5. Conclusion

Tensile tests are performed on commingled GFPP yarns. Influence of both gauge length and strain rate on the yarn tensile behavior are investigated. A significant increase of breaking strength with increasing strain rate is observed. Young's modulus of GFPP yarns is close to 30GPa. It seems to increase slightly with strain rate and decrease slightly with gauge length. Tests performed on yarns extracted from a 3D fabric show the influence of weaving on the stress-strain behavior of yarns: a significant decrease of breaking strength for yarns in both weft and warp direction is highlighted. Weft yarns were found to be the most damaged with also a decrease of Young's modulus of 17%. Using experimental results and taking into account the particular commingled yarns structure, a model is proposed to describe the GFPP yarns tensile behavior. The model allows describing accurately the full average stress-strain tensile behavior.

Acknowledgments

The research leading to these results has received funding from the European Union Seventh Framework Programme (*FP7/2007-2013)* under grant agreement n° 263223.

References

[1] S. Allaoui, G. Hivet, D. Soulat, A. Wendling, P. Ouagne and S. Chatel "Experimental preforming of highly double curved shapes with a case corner using an interlock reinforcement ", International Journal of Material Forming, 2012, DOI: 10.1007/s12289-012-1116-5..

[2] R.H.W. ten Thije, R. Akkerman, "A multi-layer triangular membrane finite element for the forming simulation of laminated composites" Composites: Part A, 2009; 40:739–753.

[3] J. S. Lightfoot, M. R. Wisnom, K. Potter; "Defects in woven preforms: Formation mechanisms and the effects of laminate design and layup protocol" Composites: Part A 51 (2013) 99–107.

[4] Torun A. R. Advanced manufacturing technology for 3D profiles woven performs. Phd thesis.

[5] P. Kravaev, O. Stolyarov, G. Seide, T. Gries. Influence of process parameters on filament distribution and blending quality in commingled yarns used for thermoplastic composites. Journal of thermoplastic composite materials 1-14. 2012.

[6] R. Alagirusamy, Vinayak Ogale. Development and characterization of GF/PET, GF/Nylon, and GF/PP commingled yarns for thermoplastic composites. Journal of thermoplastic composites materials 2005 18:269.

[7] V. Ogale, R. Alagirusamy. Tensile properties of GF-polyester, GF-nylon, and GF-polypropylene commingled yarns. Journal of the textile institute 2007 Vol. 98 No. 1 pp. 37-45.

[8] M. Fazeli, R. Kleicke, C. Cherif, W. V. Paepegem. High-performance lightweight multifunctional composites based on 3D-shaped multilayered woven fabrics. 4th world conference on 3D fabrics and their applications, Proceedings. P. 1-12.

[9] R. Chudoba. Effect of twist, fineness, loading rate and length on tensile behavior of multifilament yarns (A multivariate study). Textile Research Journal Vol 77(11): 880-891.
[10] W. Weibull. A statistical distribution of wide applicability. Journal of applied mechanics. September, 1951.
[11] Z. Chi, TW. Chou, G. Shen. Determination of single fibre strength distribution from fibre bundle testings. Journal of materials science 19 (1984) 3319-3324.
[12] Z. Wang, Y. Xia. Experimental evaluation of the strength distribution of fibers under high strain rates by bimodal Weibull distribution. Composites Science and Technology 57 (1997) 1599-1607.
[13] R. Chudoba, M. Vorechovsky, M. Konrad. I. Random properties within the cross-section and size effect. International journal of solids and structures 43 (2006) 413-434.
[14] L. Lee, S. Rudov-Clark, A.P. Mouritz, M.K. Bannister, I. Herszberg. Effect of weaving damage on the tensile properties of three-dimensional woven composites. Composite Structures 57 (2002) 405-413.